NUCLEAR INSTRUMENTS AND METHODS 104 (1972) 455–459; © NORTH-HOLLAND PUBLISHING CO.

CONVERSION ELECTRON SPECTRA*

A line shape analysis for permanent magnet spectrographs

C. DIETHRICH† and M. L. WIEDENBECK

Department of Physics, University of Michigan, Ann Arbor, Michigan, U.S.A.

Received 23 May 1972

A computer analysis of the line shapes for semi-circular magnetic spectrographs has been carried out for a wide variety of parameters. New information on the optimum positioning of the photographic plate for given source and slit configurations has been obtained. The utility of a wide source, narrow slit configuration is pointed out.

1. Introduction

Magnetic spectrometer measurements were the primary means for determining gamma-ray energies until the development of scintillation spectrometers in 1948. While later instrumental developments have substantially reduced their importance, semicircular permanent magnetic spectrometers are still far from obsolete. The complete exploitation of the virtues of these devices depends on detailed understanding of the "shape" of the recorded lines, i.e. the intensity distribution of the electron beam where it strikes the emulsion or other detector. A detailed investigation of line shapes was carried out, by computer analysis, to provide a complete solution of the full three-dimensional problem. In particular, it is now known in detail how a line shape can be changed by variations in source width and height, slit width, source-slit-plate orientation and election trajectory radius. The results of the computer analysis were verified by the study of a number of conversion lines in the decay of ^{109}Cd, ^{140}La and ^{192}Ir.

* Supported in part by the U.S. Atomic Energy Commission and by the National Science Foundation.

† Now at St. Vincent College, Latrobe, Pennsylvania, U.S.A.

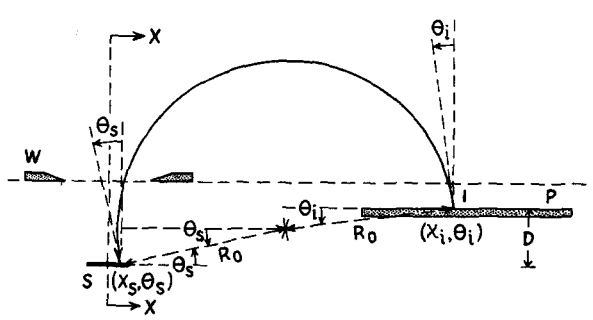

Fig. 1. Schematic for the source-to-image transformation.

2. Analysis of line shapes

The spectrometers considered are of the "flat type" which employ transverse focusing, forming line images of point sources with aberrations analogous to second-order aberrations in optical instruments. Of the many studies of line profiles, the papers by Owen[1]) and by Fowler et al.[2]) are of greatest interest. The latter, overlooked in Siegbahn's[3]) summary of earlier elegant and complicated schemes, provides the starting point for this further investigation. The treatment of the two-dimensional+ problem by Fowler et al. is an *exact*, though graphical one.

Fig. 1 shows a single circular trajectory for a particle projected at an angle θ_s from a point x_s on the line source. The corresponding coordinates θ_i and x_i specify the point "image", i.e. the intersection of the trajectory with the photographic plate. Using the notation in fig. 1, the following relations are evident:

$$\theta_s = \sin^{-1}(D/R_0 - \sin\theta_i),$$

$$x_s = x_i - R_0\cos\theta_i - R_0[1-(D/R_0-\sin\theta_i)^2]^{\frac{1}{2}}.$$

The Jacobian of the transformation from source to image coordinator is

$$J\left(\begin{smallmatrix} x_s\theta_s \\ x_i\theta_i \end{smallmatrix}\right) = \frac{-\cos\theta_i}{[1-(D/R_0-\sin\theta_i)^2]^{\frac{1}{2}}},$$

and for isotropic source emission intensity I_0, the

+ "Two-dimensional case" refers to the situation in which one assumes: all electrons which contribute to the line shape have their trajectories confined to the median plane, perpendicular to the magnetic field. This is a good approximation for a source of small height provided one considers only the region of the line shape close to the center-line of the photographic plate. "Three-dimensional case" corresponds to the real experimental situation of a source ribbon of non-negligible height.

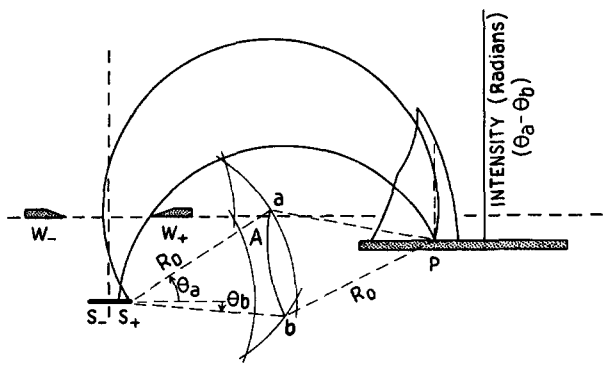

Fig. 2. Construction of the two-dimensional line shape.

image intensity $I(x_i, \theta_i)$ satisfies the equation

$$I(x_i, \theta_i)\, dx_i d\theta_i = I_0 dx_s d\theta_s = I_0 J\left(\frac{x_s \theta_s}{x_i \theta_i}\right) dx_i d\theta_i .$$

Integration yields the image density

$$V_{(x_i)} = I_0 \sin^{-1}(D/R_0 - \sin\theta_i) = I_0(\theta_a - \theta_b),$$

where θ_a and θ_b are the limiting angles for the trajectories. Fig. 2 shows the intersections of four circles of radius R_0, centered at S+, S−, W+, W−, and defines an area A which contains the center of all circular trajectories which can originate from the source and get through the slit. To determine the intensity V_{x_i} at some point P on the image, construct another circle of radius R_0 with P at its center. The intersections a and b of this circle with the perimeter of the area A determine the limiting angles θ_a and θ_b whose difference then gives the relative intensity at P.

From the previous description, the two-dimensional algorithm for the computer program is developed as follows:

1) For a given disposition of source, slit and plate, the perimeter of A is established and the leading and trailing edges of the image are located.
2) The established image width is divided into 100 equal intervals which constitute the point-by-point scan of the whole shape. At each step the angular spread $\theta_a - \theta_b$ is established.
3) The output $(\theta_a - \theta_b)$ is plotted as a function of position on the plate and the total area under the line profile is calculated.

The IBM 7090 was programmed to carry out the procedures outlined above, but for a thorough yet rapid survey of hundreds of assorted combinations of parameters it was convenient to have access to immediate graphic display of the output such as provided by the DEC PDP-1. It was then possible to feed in step-wise variations of any single parameter and observe the resulting changes in the lineshape as it was displayed on the cathode-ray tube.

3. Results

For the two dimensional treatment with the source symmetrically positioned with respect to the perpendicular bisector of the slit opening:

1) In the case of a point source, minimum image width is obtained with the plate in the plane of the slit.

2) For an extended source, fig. 3, the optimum intercepting position is behind the slit plane by an amount which increases with increasing source width.

3) For source and slit width equal, minimum beam width occurs midway between the source and slit plane. This prompts an immediate extension of the inquiry to the case of source width greater than slit width, a possibility surprisingly rarely considered in the past[4,5]). In order to see what happens in this case one only needs to interchange the roles of source and slit in fig. 3. Then, assuming a reversal of the magnetic field, trajectory patterns remain exactly as they were, leading to the obvious conclusion that: a) for an extended source and point slit, minimum image width is obtained with the plate in the source plane, b) for a finite slit and still wider source, optimum interception occurs a head of the source plane by an amount that increases with increasing slit width. The recognition of the complete interchangeability of the roles of source and slit can extend the use of this instrument to a wider range of problems while still maintaining its good resolution.

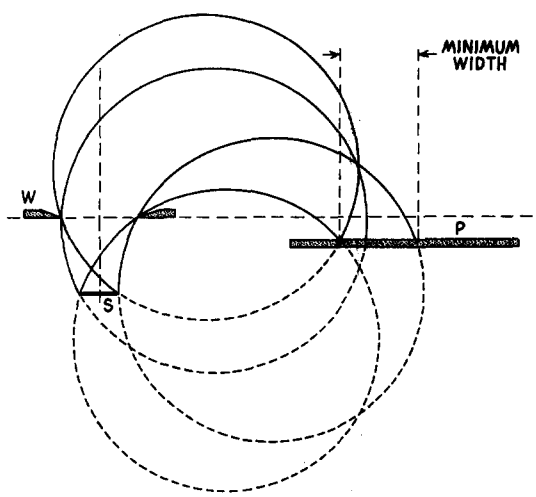

Fig. 3. Extension of finite source trajectories to illustrate optimum plate positioning and complete interchangeability of the roles of source and slit.

Several representative families of lineshapes are shown in figs. 4 and 5. Fig. 4a is produced with the plate in the slit plane, a slit width $W = 2$ mm, and with the source positioned 20 mm behind the slit. The narrowest line is produced with a source width $S = 0{,}2$ mm, while other lines are produced with S increasing in increments of 0.2 mm. The ideal shape (high and peaked) is obtained at $S \approx 0.2\ W$.

Fig. 4b is produced with the same set of source and slit configurations but has the plate in the plane midway between the source and slit. The shape steadily improves with source width until the ideal shape is reached at $S = W$.

Fig. 4c has the plate in the source plane. The shape starts poorly but steadily improves with increasing source width, gaining considerably in peak intensity with only moderate loss of resolution. This improvement can be expected to continue even for $S > W$.

Fig. 5 shows the influence of varying the slit width for a fixed source width $S = 1$ mm. Other conditions are as for fig. 4. Fig. 5a shapes are obtained with the plate in the slit plane, and with the slit width, W, varying from 0.4 mm to 4 mm in increments of 0.4 mm. Peak intensity increases rapidly with negligible loss of resolution up to $W \approx 3.2\ S$. Beyond this point excessive tailing overwhelms further intensity gains.

Fig. 5b, plate in median plane all other conditions as in fig. 5a. Steady improvement of the lineshape occurs up to $W = S$ is followed by a broadening slightly more rapid than the accompanying increase in peak intensity.

Fig. 5c, plate in source plane. The shape deteriorates rapidly as W increases.

Up to this point, the source has been symmetrically positioned with respect to the perpendicular bisector of the slit opening. The influence of a source displaced sideways is shown in fig. 6, in which all shapes are obtained for $S = 1$ mm, $W = 2$ mm, $R_0 = 100$ mm, and the source 20 mm behind the slit. Fig. 6a represents the lineshapes obtained with the plate in the plane of the

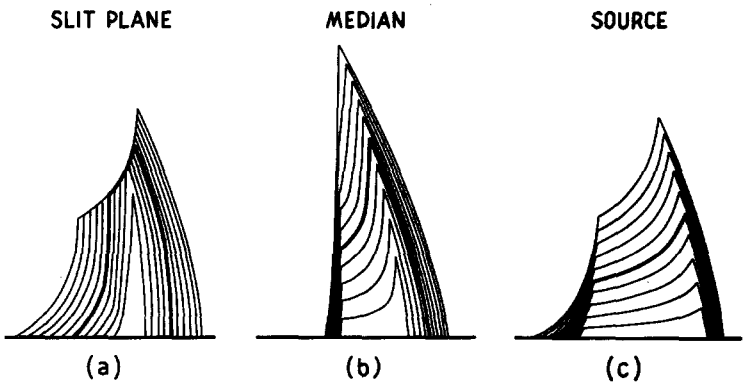

Fig. 4. Line shapes as a function of source width, $S = 0.2, 0.4, \ldots, 2.0$ mm with slit width $W = 2.0$ mm for plate in slit plane, median plane and source plane.

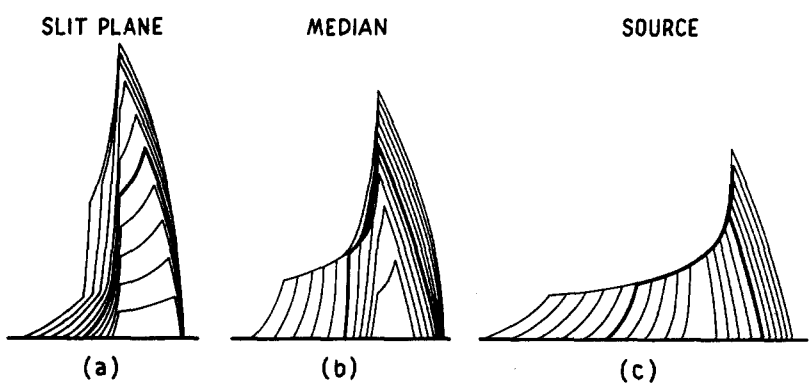

Fig. 5. Line shapes as function of slit width, $W = 0.4, 0.8, \ldots, 4.0$ mm with $S = 1.0$ mm for plate in slit plane, median plane and source plane.

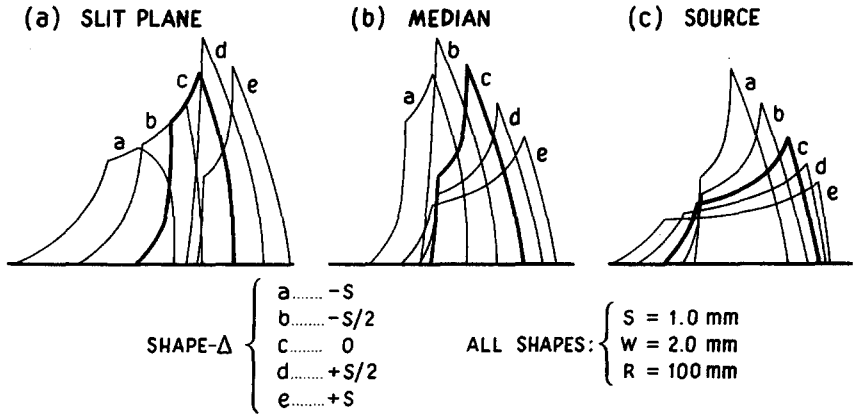

Fig. 6. Source displacement influence on line shape. Δ is displacement of source with respect to the slit bisector.

slit for various lateral positions of the source with respect to the perpendicular bisector of the slit opening. An ideal shape is produced by a rightward (toward the plate) displacement of the order of $\frac{1}{2}S$ as shown in curve d.

Figs. 6b and 6c give the corresponding line shapes for the plate in the median and source planes respectively. In the median plane the ideal shape (curve b) is obtained for a leftward shift of the source by a value $\approx \frac{1}{2}S$. With the plate in the source plane an ideal shape is not reached until the source is shifted to the left by a distance $> S$, while there is surprisingly little shift of the shape centroid for a large displacement of the source.

A significant and disturbing feature of the shapes is that they seem in most cases, to have no handy reference point which remains stationary as the several parameters are charged. Of particular importance is the fact that even for a fixed source, slit, and plate arrangement the characteristic points of the image (peak, leading edge, etc.) will vary with the trajectory radius.

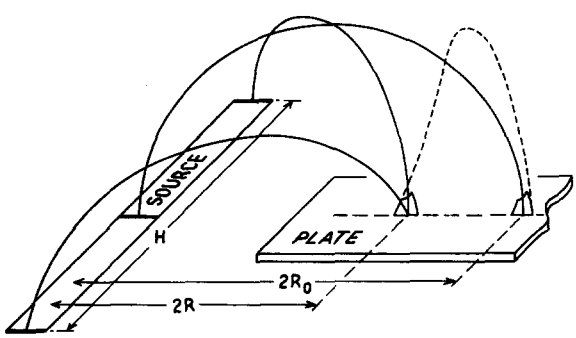

Fig. 7. Composition of the three-dimensional line shape for a long ribbon source. Trajectories are shown from filaments at the center and ends of the source to the plate centerline.

One notable exception is that in which $S = W$ with the plate in the median plane for which the ideal shape persists for *all* values of R_0.

4. Extension to the three-dimensional case

The above conclusions pertain to the two-dimensional case in which one only considers those electrons confined to the mid-plane perpendicular to the magnetic field. In practice the source is a ribbon whose height H is much greater than its width S. The line shape produced at the centerline of the plate includes contributions from above and below the centerline of the source. The trajectories are helices of radius $R = R_0[1-(z/\pi R_0)^2]^{\frac{1}{2}}$, where R_0 is the radius of the two-dimensional trajectories and z is the distance from the source centerline at which the electron originates. The full three-dimensional line shape is constructed as a superposition of appropriately displaced two-dimensional shapes (fig. 7). The source is to be treated as composed of a large number of horizontal "filaments" of width S displaced from the central plane by an amount $\pm z$, where z goes from zero to $\frac{1}{2}H$. The following results are immediately evident:

1) The disappearance of sharp discontinuities and a line base broadening will be greatest at small values of R_0, but substantial shape changes do not occur for the centerline image until $H > \frac{1}{3}R_0$. This means that, in practice, the essential conclusions reached for the two-dimensional case still apply over a wide range.

2) A pronounced increase in peak area is achieved with very little loss of resolution.

3) The full image shows the well known curvature, concave toward the source with a decreased resolution as one moves away from the centerline image.

5. Discussion

A consideration of the results of the line shape analysis leads to the following conclusions:

1) In view of the complete equivalence of the $S \ll W$, plate-in-slit plane and $S \gg W$, plate-in-source plane configurations, a decision in favor of the latter will generally be indicated by practical considerations (namely, ease of production of a wide source and a lesser dependence of image location on exact source positioning for precision energy measurements).

2) For studies in which line shape independence of electron energy is more important than combined intensity-resolution requirements, the $S = W$, plate-in-median plane configuration should be used.

3) Additional studies of the results to be expected from special "tricks", such as source shaping and tilting of photographic plate, indicate that the meager improvements provided by such techniques are completely outweighed by the difficulties they introduce.

References

1) G. E. Owen, Rev. Sci. Instr. **20** (1949) 916.

2) C. M. Fowler, R. G. Schreffler and J. M. Cork, Rev. Sci. Instr. **20** (1949) 966.

3) H. Siegbahn, *Alpha-, beta-, and gamma-ray spectroscopy*, vol. 1, ch. III (ed. K. Siegbahn; North-Holland Publ. Co., Amsterdam, 1965) p. 79.

4) H. Robinson, Proc. Roy. Soc. **104A** (1923) 455.

5) E. Persico and C. Geoffrion, Rev. Sci. Instr. **21** (1950) 945.